

# Surface Acoustic Wave Propagation Characteristics in c-plane (0001) and a-plane (11-20) AlScN Thin Films

Niclas M. Feil, Department of Sustainable Systems Engineering (INATECH), University of Freiburg, Germany  
Björn Christian, University of Freiburg, Germany  
Oliver Ambacher, University of Freiburg, Germany

## Introduction

In order to increase the data rate in the new 5G mobile communication by a factor of ten, it is necessary to access new high-frequency bands (RF bands). Therefore, new high-efficient electro-acoustic filter devices have to be developed, which operate in the high frequency ranges up to 5 GHz. The typical devices used for this application are so called surface acoustic wave (SAW) devices and bulk acoustic wave (BAW) devices. Aluminum nitride (AlN) is a common material for filter components; by substitution of Al-Atoms with Sc-Atoms, the piezoelectric performance can be significantly increased. The resulting ternary wurtzite-type nitride crystal (AlScN) is known for its large elastic and piezoelectric constants and thus is a favorable material for applications in novel RF components and therefore is promising to fit the requirements for 5G filter devices. For increasing the efficiency and bandwidth, we investigate new crystal orientations, such as a-plane AlScN on r-plane  $\text{Al}_2\text{O}_3$  (AlScN(11-20)/ $\text{Al}_2\text{O}_3$ (1-102)). The surface acoustic wave (SAW) propagation properties of AlScN(0001)/ $\text{Al}_2\text{O}_3$ (0001) and AlScN(11-20)/ $\text{Al}_2\text{O}_3$ (1-102) are analyzed using finite element method (FEM) simulations and the results are compared.

## SAW Resonator Model

Electro-acoustic filter devices are based on acoustic resonators. In case of a SAW resonator structures electrodes are deposited on a piezoelectric material. These have a comb-shaped structure to act as an interdigital transducer as well as reflectors on both sides (see Figure 1). The resonance frequency is defined by the finger pitch of the transducer structure (see Figure 2). Only applied electrical signals matching frequencies can pass through this acoustic resonator. By combining several of those resonators, band pass filters for mobile communication can be realized. Typically, these devices are characterized by vector network analyzer (VNA).

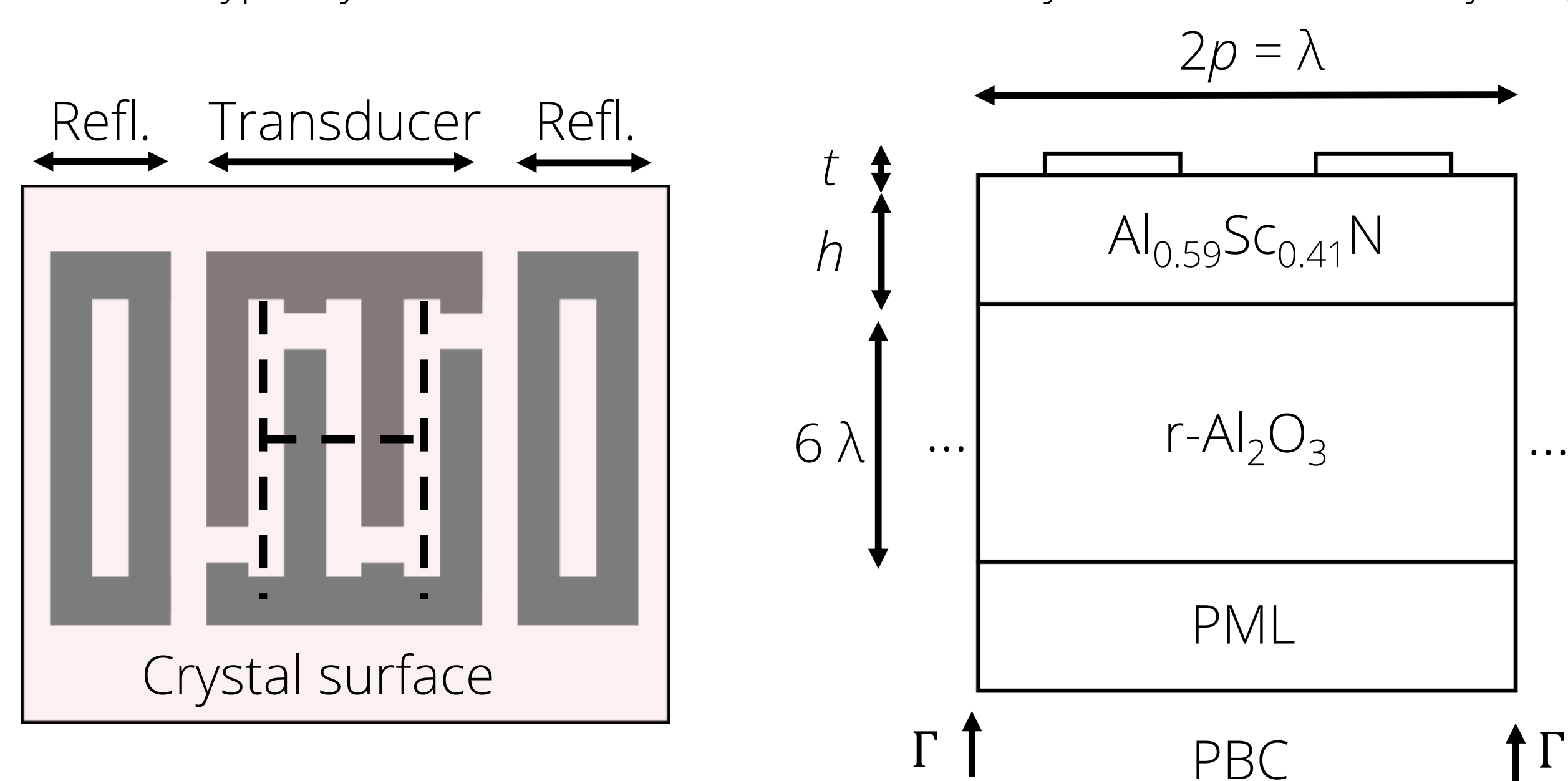


Figure 1 SAW device top view

Figure 2 FEM model geometry

## Epitaxial Relationship

For the investigation of the acoustic properties of crystals, the orientations of the respective materials in the model need to be taken into account, i.e. the crystallographic axes of the thin film and the substrate have to be transformed into new coordinate systems. In this work, the orientations are represented as Euler angles [1], defined by three angles with corresponding rotations around the new axis. In a global coordinate system for the FEM study, the wave propagation direction is defined as  $x_1$  and the surface normal as  $x_3$ . The orientations for the AlScN(0001)/ $\text{Al}_2\text{O}_3$ (0001) system are transformed according to the coincidence site lattice stacking of the two crystals, resulting in the Euler angles  $(0^\circ, 0^\circ, 0^\circ)$  for AlScN(0001) and  $(30^\circ, 0^\circ, 0^\circ)$  for  $\text{Al}_2\text{O}_3$ (0001) [2]. In the case of AlScN(11-20)/ $\text{Al}_2\text{O}_3$ (1-102), an ideal relationship of the a-plane for AlScN with the r-plane of  $\text{Al}_2\text{O}_3$  is assumed [2], illustrated in Figure 3. This leads to the Euler angles  $(90^\circ, -90^\circ, 90^\circ)$  for AlScN(11-20) and  $(-60^\circ, 57.3^\circ, 90^\circ)$  for  $\text{Al}_2\text{O}_3$ (1-102), respectively.

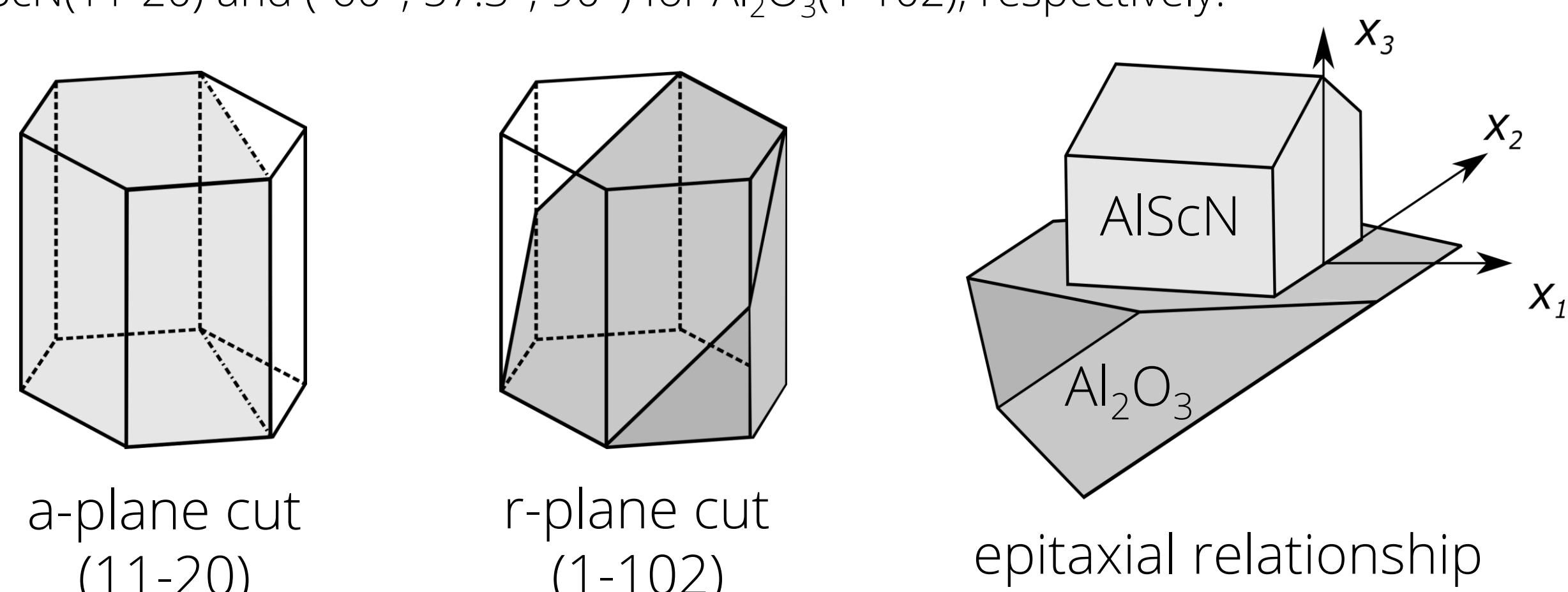


Figure 3: Crystallographic orientations of thin film and substrate. The a-plane cut for AlScN (thin film), r-plane cut for  $\text{Al}_2\text{O}_3$  (substrate) and epitaxial relationship between thin film and substrate.

## Finite Element Method (FEM) Analysis

Acoustic properties can be computed using a 2D FEM model. Periodicity of the interdigital transducer in SAW resonators allows the use of periodic boundary condition PBC (see Figure 2) from the left and right of the modeled structure. The AlScN film thickness is set to  $h_{\text{AlScN}} = 1 \mu\text{m}$  and the remaining geometrical parameters are defined as a function of the wavelength. A perfectly matched layer PML (see Figure 2) at the lower edge is defined to avoid reflection of waves at the lower part of the model. The normal modes of the defined geometry are computed for wave-lengths between 1 to 10  $\mu\text{m}$  for the 1<sup>st</sup> (Rayleigh-type) and the 2<sup>nd</sup> (Sezawa-type) wave mode. The phase velocity  $v_{\text{phase}}$  and electro-mechanical coupling  $k_{\text{eff}}^2$  are then estimated.



Figure 4: Exemplary eigenmodes of motion for antisymmetric Rayleigh-type (1<sup>st</sup>) and Sezawa-type (2<sup>nd</sup>) wave modes with  $u$ : total displacement.

## Comparison of AlScN Orientations

The comparison between c-plane  $\text{Al}_{0.59}\text{Sc}_{0.41}\text{N}$  and a-plane  $\text{Al}_{0.59}\text{Sc}_{0.41}\text{N}$  films with respect to  $v_{\text{phase}}$  and  $k_{\text{eff}}^2$  is shown in in Figure 5a and Figure 5b, respectively. The Rayleigh-type and the Sezawa-type wave mode is indicated by the circles and triangles, respectively. The phase velocity for both orientations is quite similar and shows nearly the same dispersion for c-plane and a-plane AlScN. In Figure 4a, the coupling of the 1<sup>st</sup> mode reaches its maximum of approximately  $k_{\text{eff}}^2 = 1.8 \%$  at  $h_{\text{AlScN}}/\lambda = 0.4$ , while the 2<sup>nd</sup> order waves have an increased coupling of about  $k_{\text{eff}}^2 = 4 \%$  at  $h_{\text{AlScN}}/\lambda = 0.85$ . In comparison, the properties of a-plane  $\text{Al}_{0.59}\text{Sc}_{0.41}\text{N}$  in Figure 5b show improved acoustic characteristics: The electromechanical coupling for waves of 1<sup>st</sup> mode increases to  $k_{\text{eff}}^2 = 5.8 \%$  at  $h_{\text{AlScN}}/\lambda = 0.2$ . Please note that both the values of  $k_{\text{eff}}^2$  and  $v_{\text{phase}}$  are large, which is of advantage for next generation RF-filters. On the other side, waves of the 2<sup>nd</sup> mode exhibit increased coupling in a long wavelength range, the phase velocities reach approximately  $v_{\text{phase}} = 6 \text{ kms}^{-1}$  with  $k_{\text{eff}}^2 = 6.2 \%$  at  $h/\lambda = 0.4$ . The observed high  $v_{\text{phase}}$  lead to high operation frequencies, while the increased  $k_{\text{eff}}^2$  increases the bandwidth. This is beneficial for the design of novel piezo-acoustic filter components.

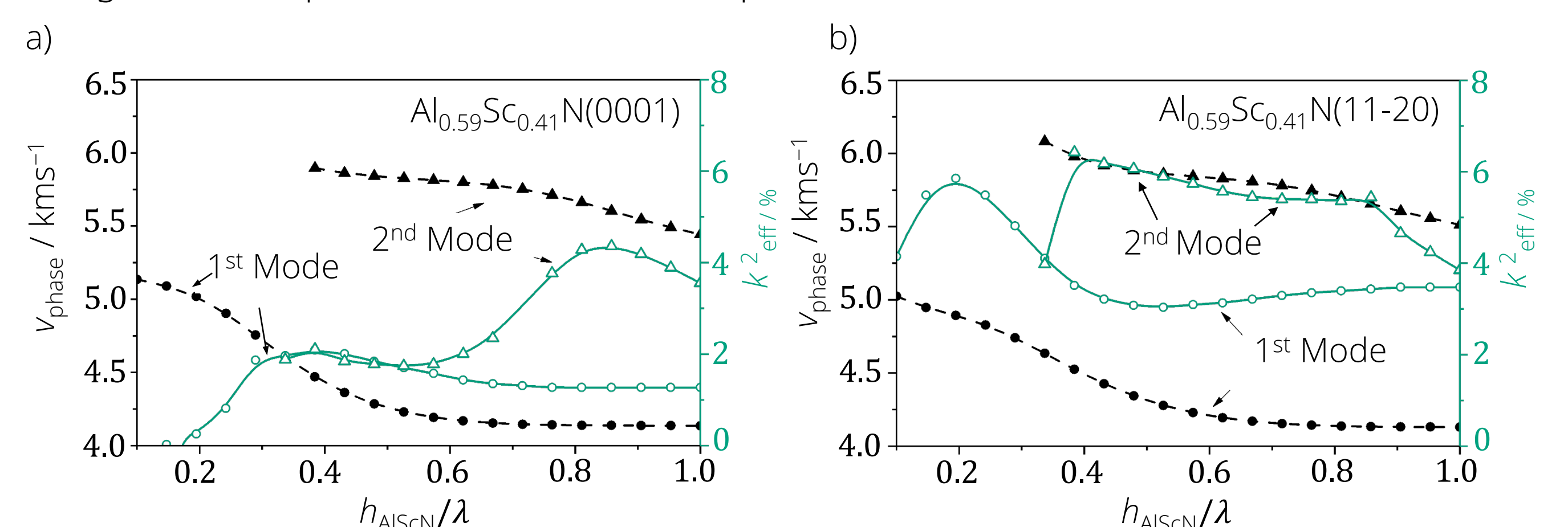


Figure 5: FEM results for different  $\text{Al}_{0.59}\text{Sc}_{0.41}\text{N}/\text{Al}_2\text{O}_3$  orientations with normalized electrode thickness  $q_{\text{Cu}} = 0.04$ . Comparison of phase velocity and electromechanical coupling coefficient with 1<sup>st</sup> and 2<sup>nd</sup> mode for a)  $\text{Al}_{0.59}\text{Sc}_{0.41}\text{N}(0001)$  and b)  $\text{Al}_{0.59}\text{Sc}_{0.41}\text{N}(11-20)$  films.

## Summary and Conclusion

The material AlScN proves to be a highly suitable candidate for future piezo-acoustic filter devices. In this work, two different orientations of wurtzite-type AlScN have been studied. For AlScN(11-20)/ $\text{Al}_2\text{O}_3$ (1-102) we have shown a high  $k_{\text{eff}}^2$  and  $v_{\text{phase}}$  at the same time. The analysis of different wave modes have shown a tripling of  $k_{\text{eff}}^2$  for the 2<sup>nd</sup> wave mode, which gives more design options for novel high frequency filters.

## References

- [1] H.J. Bunge, Texture analysis in materials science: mathematical methods. Butterworth and Co, 1982.
- [2] K. Dovidenko, S. Oktyabrsky, J. Narayan, "Aluminum nitride films on different orientations of sapphire and silicon" *J. Appl. Phys.* **79**, 2439 (1996)